

Synthesis and Characterization of Dendritic Star-Shaped Poly(ϵ -caprolactone)-*block*-Poly(L-lactide) Block Copolymers

Weian Zhang,¹ Sixun Zheng,¹ Qipeng Guo²

¹Department of Polymer Science and Engineering, Shanghai Jiao Tong University, 800 Dongchuan Road, Shanghai 200240, People's Republic of China

²Centre for Material and Fibre Innovation, Deakin University, Geelong, Victoria 3217, Australia

Received 5 June 2006; accepted 28 February 2007

DOI 10.1002/app.26484

Published online 21 June 2007 in Wiley InterScience (www.interscience.wiley.com).

ABSTRACT: Dendritic star-shaped poly(ϵ -caprolactone)-*block*-poly(L-lactide) (PCL-*b*-PLLA) diblock copolymers were synthesized via sequential ring-opening polymerization. In the first step, an aliphatic dendritic polyester containing 16 terminal hydroxyl groups was used as the core molecule to initiate the ring-opening polymerization of ϵ -caprolactone, which was catalyzed by stannous(II) octanoate, to obtain dendritic star-shaped poly(ϵ -caprolactone) (PCL) terminated with hydroxyls, which was used further to initiate the ring-opening polymerization of L-lactide to form the dendritic star-shaped diblock copolymers. The dendritic star-shaped polymers (PCL-*b*-PLLA) were characterized with nuclear magnetic resonance spectroscopy and gel permeation chromatography. The results showed that the arm length of the dendritic star-shaped polymers could be well controlled in terms of the molar ratios of the initiators (i.e., the aliphatic dendritic polyester and star-shaped

PCL) to the monomers (i.e., ϵ -caprolactone and L-lactide). The crystalline structure and thermal properties of the dendritic star-shaped polymers were investigated with X-ray diffraction and differential scanning calorimetry. The X-ray diffraction indicated that the formation of the dendritic star-shaped topological structure did not affect the structure of the crystals of PCL and poly(L-lactide) (PLLA) blocks. The thermal analyses showed that the crystallization rate of the PCL blocks in the block copolymers was greatly reduced compared to that in the parent dendritic star-shaped PCL. This observation could be attributed to the confinement of the dendritic core and PLLA blocks upon the crystallization of the PCL blocks. © 2007 Wiley Periodicals, Inc. *J Appl Polym Sci* 106: 417–424, 2007

Key words: biocompatibility; biodegradable; block copolymers; branched; polyesters

INTRODUCTION

Aliphatic polyesters such as poly(L-lactide) (PLLA) and poly(ϵ -caprolactone) (PCL) are a class of important polymer materials. Because of their biodegradability and biocompatibility, these materials represent interesting candidates for a variety of biomedical applications.^{1–15} However, these materials have some inherent drawbacks. For instance, PLLA generally possesses a high crystallinity and a low rate of degradation, which greatly limit its use in drug release systems.^{16,17} Therefore, structural modifications are required before it can be successfully applied. It is recognized that the blending and copolymerization

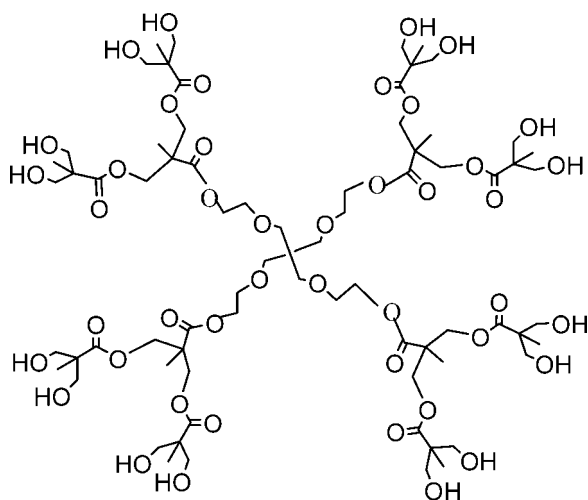
of PLLA with other polymers are efficient approaches to suppress the crystallization of PLLA and thus to enhance the rate of degradation.^{18–22} More recently, it has been found that the formation of some macromolecular topologies such as hyperbranched and star-shaped structures is also favorable for promoting the applicability of PLLA.^{23–28} However, there are only a few reports on the preparation of star-shaped block copolymers involving PLLA and PCL.^{29,30} Dendritic polymers with functional groups can be used as cores to prepare dendritic star-shaped polymers via so-called core-first^{31–37} and arm-first^{38–40} approaches. The core-first approach has been proved to be efficient for synthesizing dendritic star-shaped aliphatic polyesters such as PLLA and PCL via sequential ring-opening polymerization.^{41,42} Recently, Gedde et al.⁴³ synthesized star-shaped PCL, using dendrimer, hyperbranched, and dendron cores, and studied the crystallization behavior of the star-shaped polymers. Xi and coworkers^{18,44} used hydroxyl-terminated poly(amidoamine) and poly(aryl ether) dendrimers to prepare dendritic star-shaped PLLAs and PLLA copolymers with various arm lengths. To the best of our knowledge, there

Correspondence to: S. Zheng (szheng@sjtu.edu.cn).

Contract grant sponsor: Natural Science Foundation of China; contract grant number: 20474038.

Contract grant sponsor: Shanghai Educational Development Foundation, People's Republic of China (through an Award for Shuguang Scholars to S.Z.); contract grant number: 2004-SG-18.

Journal of Applied Polymer Science, Vol. 106, 417–424 (2007)
© 2007 Wiley Periodicals, Inc.



Scheme 1 Structure of Boltorn H20.

is no previous report on the preparation of dendritic star-shaped poly(ϵ -caprolactone)-*block*-poly(L-lactide) (PCL-*b*-PLLA) block copolymers.

In this work, we report the synthesis of novel dendritic star-shaped PCL-*b*-PLLA block copolymers; the core molecule used in this synthesis is an aliphatic dendritic polyester terminated with 16 primary alcohol hydroxyls (Scheme 1). To this end, the ring-opening polymerizations of ϵ -caprolactone (CL) and L-lactide (LLA) were carried out in separate steps to afford blocks of PCL and PLLA, respectively. The structures of the crystals and thermal properties of the dendritic star-shaped block copolymers were addressed with wide-angle X-ray diffraction (XRD) and differential scanning calorimetry (DSC).

EXPERIMENTAL

Materials

LLA was kindly supplied by Shanghai Newgenius Biotech Co., Ltd. (China). Before its use, LLA was recrystallized with anhydrous ethyl ester and dried *in vacuo* at room temperature for 24 h. CL was purchased from Fluka (Germany) and distilled over CaH_2 under decreased pressure. The aliphatic dendritic polyester was obtained from Perstorp Specialty Chemicals (Sweden) under the trade name of Boltorn H20, and it had a quoted number-average molecular weight (M_n) of 1747 g/mol and 16 terminal hydroxyl groups; its dendritic structure is shown in Scheme 1. Stannous(II) octanoate [$\text{Sn}(\text{Oct})_2$] was chemically pure, was purchased from Shanghai Reagent Co. (Shanghai, China), and was used as received. Solvents such as chloroform, tetrahydrofuran (THF), petroleum ether, and toluene were obtained from commercial sources. Before its use, toluene was puri-

fied by distillation over CaH_2 . All the reagents without special specifications were obtained from Shanghai Reagent Co.

Synthesis of dendritic star-shaped PCL

The desired amount of Boltorn H20 was charged into a round-bottom flask equipped with a dry magnetic stirring bar. This flask was connected to a Schlenk-line system and was degassed and then refilled with highly pure nitrogen. The exhausting-refilling process was repeated three times before the liquid reagent was added. The catalyst in the toluene solution was added to the system in terms of the [$\text{Sn}(\text{Oct})_2$]/[CL] ratio of 1/1000 (w/w). The polymerization was carried out at 120°C for 24 h. The crude product was dissolved in dichloromethane and precipitated with excessive petroleum ether. The precipitates were dried *in vacuo* at 45°C for 24 h.

Syntheses of dendritic star-shaped PCL-*b*-PLLA block copolymers

The aforementioned dendritic star-shaped PCL terminated with hydroxyl groups was used as the macromolecular initiator of the ring-opening polymerization of LLA to prepare the dendritic star-shaped PCL-*b*-PLLA block copolymers. The desired amounts of the dendritic star-shaped PCL and LLA were added to a flask equipped with a dried magnetic stirrer, which was connected to a Schlenk-line system for drying the reactive system with the aforementioned procedure. The flask was immersed in an oil bath at 130°C for 24 h to access complete polymerization. The crude product was dissolved in chloroform and precipitated with excessive petroleum ether. The precipitates were dried *in vacuo* at 45°C for 24 h.

Methods and measurements

Nuclear magnetic resonance (NMR) spectroscopy

The NMR measurements were carried out on a Varian Mercury Plus 400-MHz NMR spectrometer at 25°C. The polymer was dissolved with deuterated chloroform, and the ^1H spectrum was obtained with tetramethylsilane as the internal reference.

Gel permeation chromatography (GPC)

The molecular weight and molecular weight distribution were measured on a Waters 150C gel permeation chromatograph equipped with Microstysragel columns at 35°C. THF was used as the eluent at a flow rate of 1.0 mL/min. The molecular weights were expressed with respect to a polystyrene standard.

TABLE I
Results of the Polymerization of CL with Boltorn H20 as the Initiator

Sample	[CL]/[I] ^a	$M_{n, \text{GPC}}^b$	$M_{n, \text{NMR}}^c$	$M_{n, \text{th}}^d$	M_w/M_n^b	Yield (%)
DPCL1	175/1	22,000	19,100	20,583	1.17	94.4
DPCL2	350/1	40,000	39,200	39,854	1.19	95.5
DPCL3	598/1	64,200	65,700	67,969	1.14	97.1
DPCL4	701/1	74,200	78,500	75,511	1.15	92.3

^a Molar ratio of the monomer (CL) to the initiator (Boltorn H20).

^b Determined by GPC with polystyrene standards.

^c Determined from the ¹H-NMR spectrum of dendritic star-shaped PCL.

^d Theoretical number-average molecular weight: $M_{n, \text{th}} = [\text{CL}]/[\text{I}] \times M_{\text{CL}} \times \text{Yield} + M_{\text{Boltorn H20}}$, where M_{CL} is the molecular weight of CL and $M_{\text{Boltorn H20}}$ is the molecular weight of Boltorn H20.

XRD

The XRD patterns were obtained with a Rigaku D/max γ X-ray diffractometer equipped with graphite-monochromatized Cu K α radiation ($\lambda = 0.154$ nm). The scanning range was 5–60° with a scanning rate of 2°/min.

DSC

The DSC experiments were carried out on a Perkin Elmer Pyris 1 differential scanning calorimeter in a nitrogen atmosphere. The instrument was calibrated with standard indium. The first scans were performed from –70 to 180°C at the heating rate of 20°C/min and were held at 180°C for 3 min to melt the crystals; this was followed by quick quenching to –70°C. The second heating scans were carried out from –70 to 180°C at the heating rate of 20°C/min. After that, the samples were cooled from 180 to –70°C at the cooling rate of 10°C/min, and the cooling DSC curves were recorded. The crystallization temperatures and melting temperatures were taken as the temperatures at the maximum and minimum of the endothermic and exothermic peaks, respectively.

RESULTS AND DISCUSSION

Synthesis of dendritic star-shaped PCL

In this work, the dendritic star-shaped PCL terminated with hydroxyls was first prepared, and it was used as the macromolecular initiator to initiate the polymerization of LLA to obtain the dendritic star-shaped PCL-*b*-PLLA diblock copolymers. The dendritic star-shaped PCL was synthesized via the ring-opening polymerization of CL in the presence of the aliphatic dendritic polyester (Boltorn H20). The polymerization was carried out at 120°C for 24 h with Sn(Oct)₂ as the catalyst. The four dendritic star-shaped PCLs with different molecular weight were

synthesized and denoted DPCL1, DPCL2, DPCL3, and DPCL4 (Table I). Figure 1 shows the ¹H-NMR spectrum of the dendritic star-shaped PCL (DPCL2) together with the assignment of the resonance. The resonances of protons from Boltorn H20 are discernible, indicating the occurrence of the polymerization initiated with the dendritic polyester. The resonances at 1.22 and 2.42 ppm are assigned to the protons of methyl and methylene groups of Boltorn H20, respectively. The resonances at a (4.05 ppm), b (2.31 ppm), c (1.64 ppm), d (1.38 ppm), and e (3.65 ppm) are ascribed to the protons of the PCL main chains, as indicated in Figure 1. ¹H-NMR spectroscopy indicates that the as-prepared product combined the structural features of both Boltorn H20 and PCL. The molecular weights of the dendritic star-shaped PCL were determined with GPC and ¹H-NMR spectroscopy. The results of the polymerization are summarized in Figure 2 and Table I. According to Figure 2, the molecular weights of the dendritic star-shaped PCL linearly increased with an increasing molar ratio of the monomer to the macromolecular initiator, and this implied that the molecular weight of the dendritic star-shaped PCL could be well controlled in terms of the feed ratios.

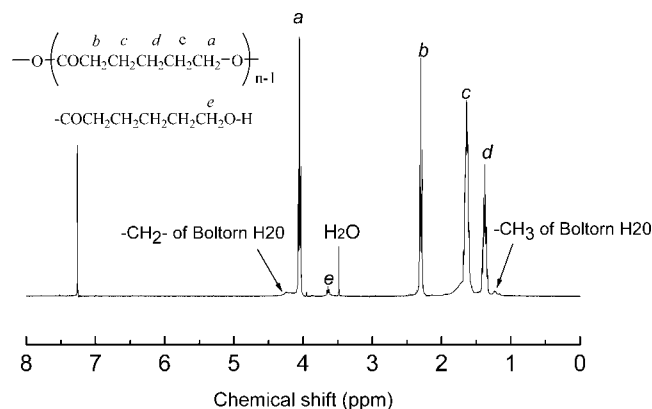


Figure 1 ¹H-NMR spectrum of dendritic star-shaped PCL (DPCL2).

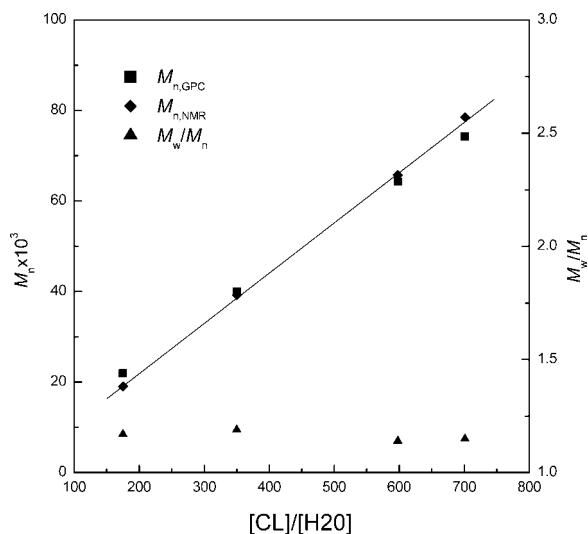


Figure 2 Dependence of the molecular weights ($M_{n,GPC}$ and $M_{n,NMR}$) and molecular weight polydispersity of dendritic star-shaped PCL on the molar ratio of CL to Boltorn H20 with Boltorn H20 as the initiator.

Synthesis of dendritic star-shaped PCL-*b*-PLLA block copolymers

One of the dendritic star-shaped PCLs (DPCL2) was further used as the macroinitiator to initiate the ring-opening polymerization of LLA, which was catalyzed by $\text{Sn}(\text{Oct})_2$. The polymerization was carried out at 130°C for 24 h to obtain products of high molecular weights. The four dendritic star-shaped PCL-*b*-PLLA diblock copolymers with different molecular weights were prepared and denoted as DPCLA1, DPCLA2, DPCLA3, and DPCLA4 (Table II). Representatively shown in Figure 3 is the $^1\text{H-NMR}$ spectrum of a dendritic star-shaped PCL-*b*-PLLA diblock copolymer (DPCLA2). The signal of the methyl protons for Boltorn H20 is still detected at 1.22 ppm in the spectrum. Nonetheless, the signal is not discernible in the $^{13}\text{C-NMR}$ spectrum, possibly because of the low ratio of the signal to the noise

(Fig. 4). Figure 3 shows that the methylene proton signals at 3.65 ppm of the PCL ($\text{HOCH}_2\text{CH}_2-$) disappeared, and the new proton signals appeared at 4.40 ppm, assignable to the terminal methine protons of PLLA [$\text{HOCH}(\text{CH}_3)-$]. This observation indicates that the dendritic star-shaped PCL-*b*-PLLA diblock copolymer was obtained. The molecular weights of the PLLA blocks were estimated from the intensity ratios of the methine proton signals (at 5.15 ppm) of PLLA to those of methylene protons (at 2.32 ppm) of PCL. The $M_{n,NMR}$ values of the copolymer are summarized in Figure 5 and Table II. Figure 5 shows that $M_{n,NMR}$ of the copolymer linearly increased with the molar ratio of LLA to the macroinitiator. Therefore, the block length of the star copolymer could be well controlled by the adjustment of the molar ratio of LLA to the macroinitiator. The molecular weights determined by GPC ($M_{n,GPC}$) for the copolymers were obviously lower than those estimated with NMR. This observation is attributed to the smaller hydrodynamic volume of the dendritic star-shaped copolymer versus that of the linear counterpart with identical molecular weights. The typical GPC curves of the block copolymers and the original block PCL are shown in Figure 6. The symmetry of the GPC curves indicates that no homopolymers were found in the dendritic star-shaped diblock copolymers, suggesting that the terminal hydroxyl groups of the star-shaped PCL macroinitiator were all involved in the polymerization of the LLA monomer.

Thermal properties

The thermal properties of the dendritic star-shaped PCL-*b*-PLLA block copolymers were investigated, and the DSC curves of the dendritic star-shaped diblock copolymers are shown in Figure 7. Shown in Figure 7(a) are the first heating scans for the as-prepared samples. For DPCL2, there was an exother-

TABLE II
Results of the Polymerization of LLA with Dendritic Star-Shaped PCL (DPCL2) as the Initiator

Sample	[LLA]/[I] ^a	$M_{n,GPC}$ ^b	$M_{n,NMR}$ ^c	$M_{n,th}$ ^d	M_w/M_n ^b	Yield (%)
DPCL2	—	40,000	39,200	39,854	1.19	95.5
DPCLA1	139/1	51,800	56,800	58,769	1.16	94.5
DPCLA2	278/1	66,400	72,900	76,764	1.16	92.2
DPCLA3	556/1	86,600	110,400	112,952	1.16	91.3
DPCLA4	833/1	104,300	143,400	148,050	1.20	90.2

^a Molar ratio of the monomer (LLA) to the initiator (DPCL2).

^b Determined by GPC with polystyrene standards.

^c Determined from the $^1\text{H-NMR}$ spectrum of the dendritic star-shaped PCL-*b*-PLLA copolymer.

^d Theoretical number-average molecular weight: $M_{n,th} = [\text{LLA}]/[\text{I}] \times M_{\text{LLA}} \times \text{Yield} + M_{n,th,DPCL2}$, where M_{LLA} is the molecular weight of LLA and $M_{n,th,DPCL2}$ is the theoretical number-average molecular weight of DPCL2.

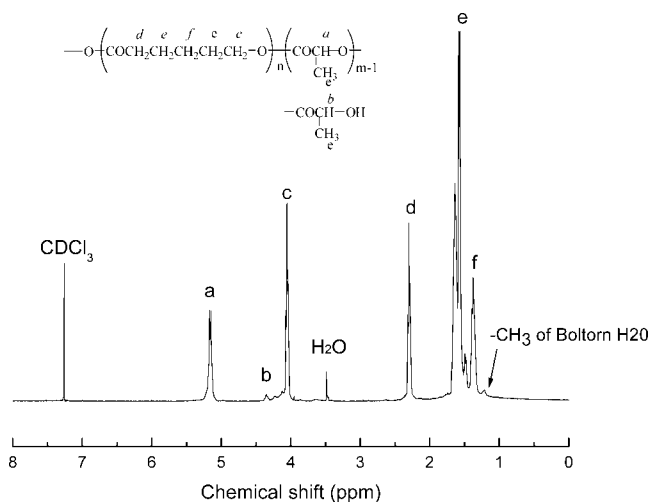


Figure 3 $^1\text{H-NMR}$ spectrum of the dendritic star-shaped PCL-*b*-PLLA block copolymer (DPCLA2).

mic transition at 61°C , which was ascribed to the melting transition of PCL. However, this transition shifted to a lower temperature in the dendritic star-shaped PCL-*b*-PLLA diblock copolymers. Furthermore, a shoulder peak appears with the melting peak, implying that the lamellar rearrangement of PCL crystals was affected by the presence of the PLLA block. With increasing molecular weights of the PLLA blocks, the melting transition of the PCL blocks became increasingly weak. For DPCLA3 and DPCLA4, the transitions were indiscernible. The observation could be interpreted as follows. First, the result could be related to the partial miscibility of PCL and PLLA. PLLA possesses a higher glass-transition temperature ($\sim 60^\circ\text{C}$) than PCL ($\sim -60^\circ\text{C}$).⁴⁵ Therefore, partially mixing the two blocks resulted in the increase in the glass-transition temperatures

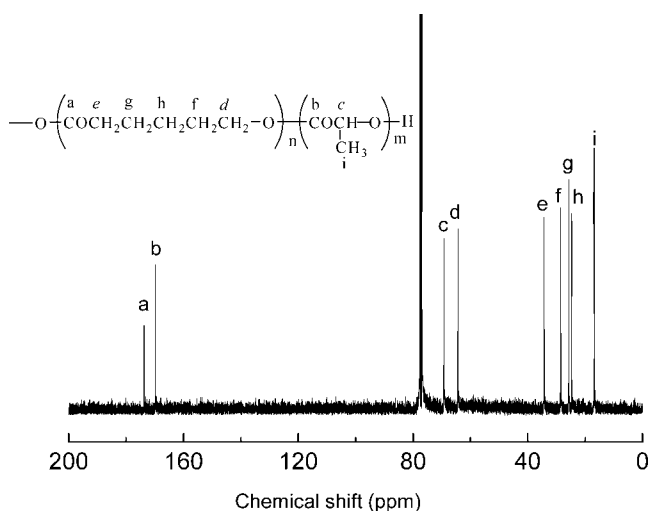


Figure 4 $^{13}\text{C-NMR}$ spectrum of the dendritic star-shaped PCL-*b*-PLLA block copolymer (DPCLA2).

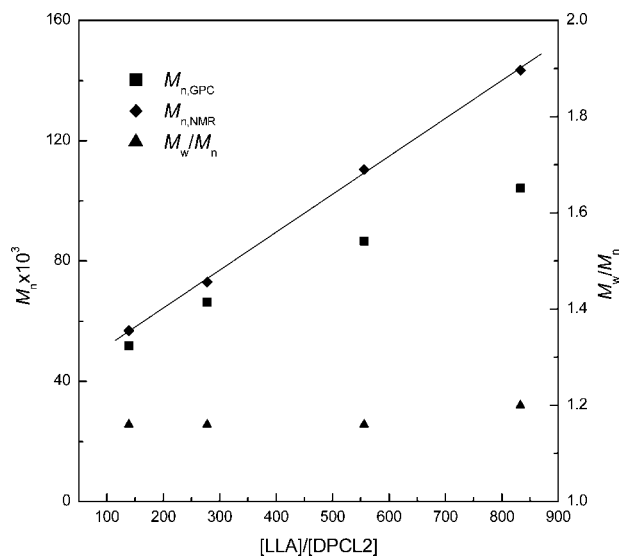


Figure 5 Dependence of the molecular weights ($M_{n,\text{GPC}}$ and $M_{n,\text{NMR}}$) and molecular weight polydispersity of dendritic star-shaped PCL-*b*-PLLA block copolymers on the molar ratio of LLA to DPCL2 with dendritic star-shaped PCL as the initiator.

for PCL domains; that is, a lower supercooling degree (melting temperature – glass-transition temperature) was created for the crystallization of PCL chains. In addition, the confined crystallization of PCL chains in the star-shaped diblock copolymers should also be considered. In the dendritic star-shaped block copolymers, the terminal ends of PCL chains were restricted by the core molecules and PLLA block, and thus the crystallization of PCL chains was significantly confined.^{46,47} It is plausible to propose that the restriction is increasingly pronounced.

The thermal properties of the PLLA blocks in the dendritic star-shaped copolymers are also shown in Figure 7(a). For DPCLA1, no melting peak assignable to PLLA appears in the DSC curve, and this suggests

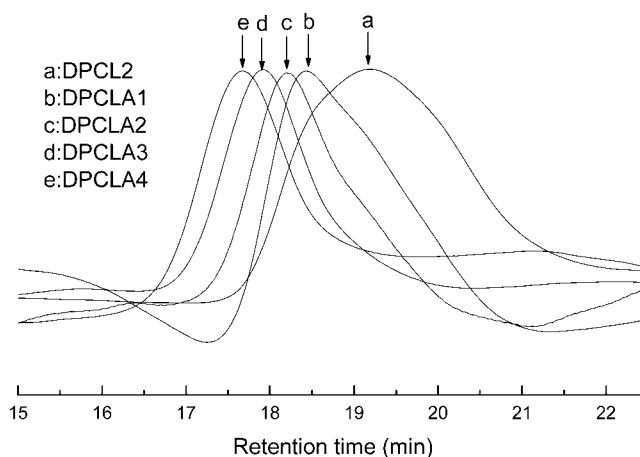


Figure 6 GPC curves of dendritic star-shaped PCL and dendritic star-shaped PCL-*b*-PLLA block copolymers.

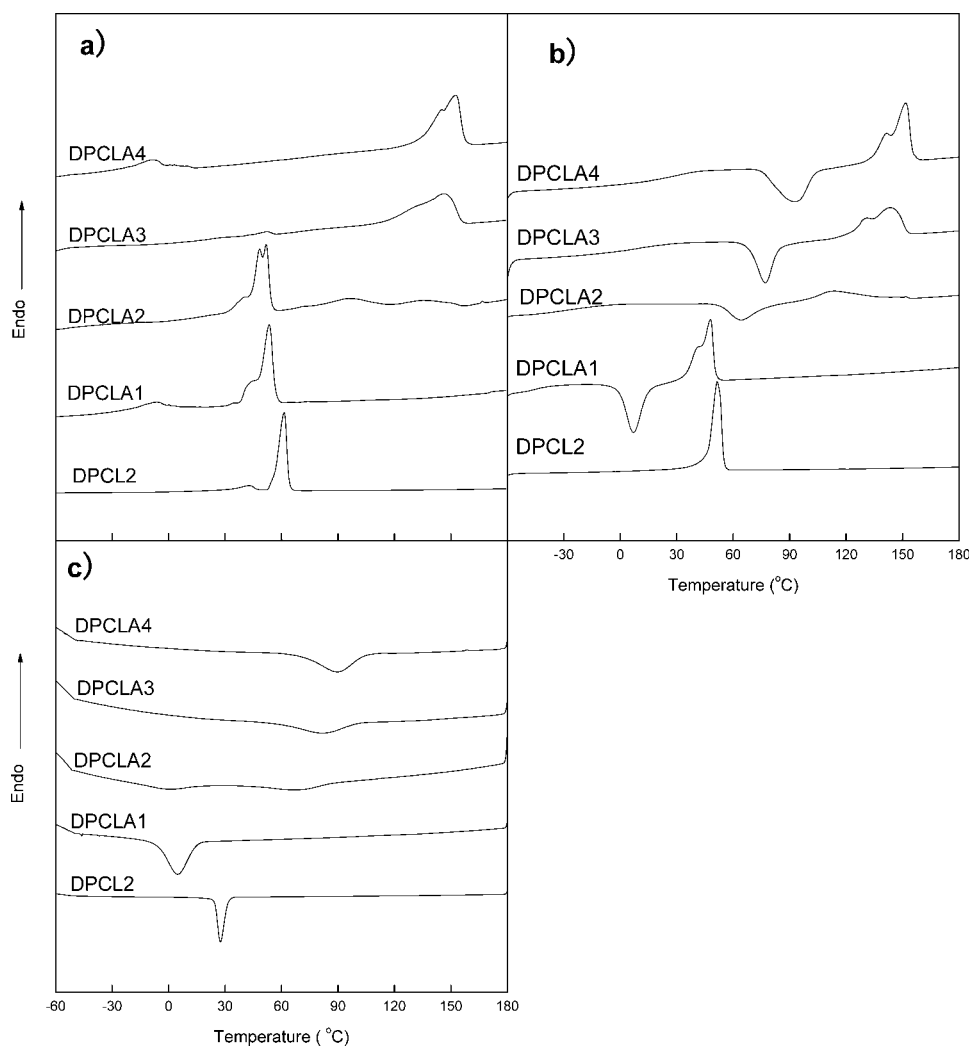


Figure 7 DSC traces of dendritic star-shaped PCL and dendritic star-shaped PCL-*b*-PLLA block copolymers: (a) first heating scan, (b) second heating scan after 3 min at 180°C, and (c) cooling scan.

that the PLLA microdomain is amorphous. Nonetheless, the crystallization of PLLA was seen when the length of the PLLA blocks was increased. For DPCLA2, there are two weak melting peaks in the DSC curve at temperatures higher than the melting temperatures of PCL blocks, suggesting the presence of PLLA crystals. The melting temperatures of the PLLA blocks increased with increasing lengths of the PLLA blocks (see DPCLA3 and DPCLA4).

After the thermal history was removed, the second DSC scans were carried out for the quenched samples [Fig. 7(b)]. For DPCL2, a single sharp melting transition was observed, which was ascribed to the melting of PCL crystals. However, with the incorporation of PLLA blocks, a cold crystallization transition at -8°C appeared for DPCLA2, suggesting that the crystallization of PCL blocks was significantly inhibited by the presence of PLLA blocks. The crystallization rates of PCL blocks decreased with

increasing lengths of PLLA blocks. For the dendritic star-shaped block copolymers with longer PLLA blocks (i.e., DPCLA3, DPCLA3, and DPCLA4), no cold crystallization or subsequent melting transitions were observed, and this implied that the crystallization rates of PCL blocks in these samples were too slow to be detected. On the other hand, the increased lengths of the PLLA blocks endowed the crystallinity of PLLA blocks. By comparing the area of the cold crystallization peak with that of the melting peak for DPCLA2, it is proposed that an amorphous sample could be obtained when the copolymer was quenched. However, the cold crystallization temperature for the PLLA blocks increased with the increasing length of PLLA blocks, whereas the melting temperatures of the PLLA blocks remained almost invariant. This observation could be related to the microphase structures of the dendritic star-shaped diblock copolymers.

The degree of crystallization (X_c) of the polymer could be calculated with the following equation:

$$X_c = (\Delta H_f - \Delta H_c) / \Delta H_f^0$$

where ΔH_f^0 is the heat of fusion of the 100% crystalline polymer, ΔH_f is the heat of fusion of the polymer, and ΔH_c is the heat of crystallization during the same heating scan. X_c of the PCL and PLLA blocks in the dendritic star-shaped block copolymers could be calculated by the equation with the DSC curves of the second heating scan. For PCL, ΔH_f^0 was 136 J/g,⁴⁸ and X_c of the PCL blocks in DPCL2 was 49.28%, but X_c in DPCLA1 was 4.37%, and this suggests that X_c of the PCL blocks greatly decreased in the dendritic star-shaped copolymer. For PLLA, X_c of the PLLA block in DPCLA2, DPCLA3, and DPCLA4 was 5.82, 9.36, and 8.67%, respectively, when ΔH_f^0 was 93.6 J/g.⁴⁹ This indicates that X_c increased with the molecular weight of the PLLA block increasing. However, when the molecular weight of the PLLA block increased to a certain value, X_c was independent of the molecular weight of the PLLA block. Thus, the crystallinity of the PLLA block could be adjusted by the variation of the molecular weight of the PLLA block.

Figure 7(c) shows the cooling scan from 180 to -70°C at $10^\circ\text{C}/\text{min}$. DPCL2 had a crystallization exotherm, and its crystallization temperature was at 28°C . For the dendritic star-shaped copolymers, the crystallization exothermic peaks of the PCL blocks appeared only for DPCLA1 and DPCLA2. Compared to that of DPCL2, the crystallization exothermic peaks of the PCL blocks shifted to lower temperatures and their intensity became weaker with the lengths of the PLLA blocks increasing. This further confirms that the crystallization of PCL blocks in the dendritic star-shaped copolymers was restricted. In addition, the temperature of the PLLA blocks increased with the length of the PLLA blocks increasing.

Structures of the crystals

Figure 8 shows the XRD patterns of the dendritic star-shaped PCL (DPCL2) and its diblock copolymers with PLLA. DPCL2 shows two strong peaks and a weak peaks at 2θ values of 21.4, 23.7, and 22.0° , which correspond to the 110, 200, and 111 planes of PCL, respectively.⁵⁰ This observation suggests that the formation of a dendritic star-shaped topology does not alter the structure of PCL crystals. The typical diffraction peaks of the PCL blocks were also found in the dendritic star-shaped diblock copolymers. A similar case is also applicable to the structure of the PLLA crystals. For PLLA blocks, the diffraction peaks were also detected at 2θ values of

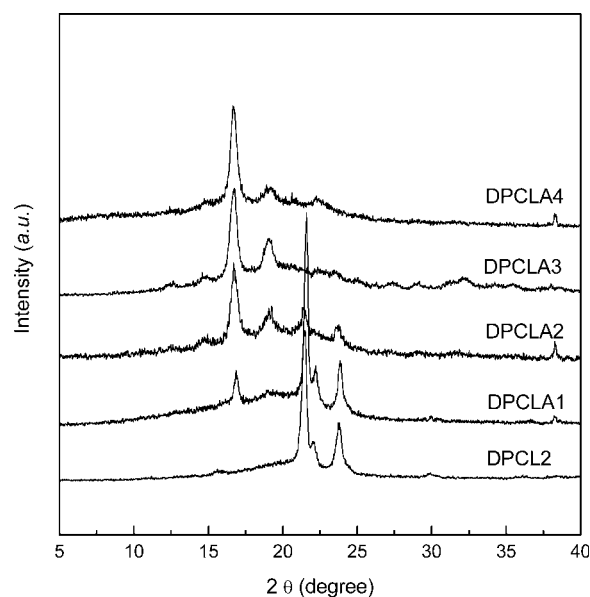


Figure 8 XRD patterns of dendritic star-shaped PCL and dendritic star-shaped PCL-*b*-PLLA block copolymers.

16.6 and 18.9° , which correspond to the 200 and 203 planes of PLLA, respectively.^{51,52} It is interesting to note the minor diffraction peak at 16.6° in the pattern of DPCLA1, suggesting low crystallinity for PLLA. However, the melting transition was not found in the DSC thermogram (Fig. 7).

CONCLUSIONS

The dendritic star-shaped PCL-*b*-PLLA block copolymers were synthesized via sequential ring-opening polymerization. In the first step, an aliphatic dendritic polyester containing 16 terminal hydroxyl groups was used as the core molecules to initiate the ring-opening polymerization of CL, which was catalyzed by $\text{Sn}(\text{Oct})_2$, to obtain the dendritic star-shaped PCL terminated with hydroxyls, which was used further to initiate the ring-opening polymerization of LLA to form the dendritic star-shaped diblock copolymers. The dendritic star-shaped polymers (PCL-*b*-PLLA) were characterized with NMR spectroscopy and GPC. The results showed that the arm length of the dendritic star-shaped polymers could be well controlled in terms of the molar ratios of the initiators (i.e., Boltorn H20 or star-shaped PCL) to the monomers (i.e., CL and LLA). The crystalline structure and thermal properties of the dendritic star-shaped polymers were investigated with XRD and DSC. XRD indicated that the formation of a dendritic star-shaped topological structure did not affect the structure of the crystals of PCL and PLLA blocks. The thermal analyses showed that the crystallization rate of the PCL blocks in the block copolymers was

greatly reduced compared to that in the parent dendritic star-shaped PCL. The observation could be attributed to the confinement of the dendritic core and PLLA blocks upon the crystallization of the PCL blocks.

References

- Uhrich, K. E.; Cannizzaro, S. M.; Langer, R. S.; Shakesheff, K. M. *Chem Rev* 1999, 99, 3181.
- Lyman, D. J.; Rowland, S. M. *Encyclopedia of Polymer Science and Engineering*, 2nd ed.; Wiley: New York, 1985; Vol. 2, p 267.
- Albertsson, A.-C.; Varma, I. K. *Biomacromolecules* 2003, 4, 1466.
- Dechy-Cabaret, O.; Martin-Vaca, B.; Bourissou, D. *Chem Rev* 2004, 104, 6147.
- Anderson, J. M.; Shive, M. S. *Adv Drug Delivery Rev* 1997, 28, 5.
- Kataoka, K.; Kwon, G. S.; Yokoyama, M.; Okano, T.; Sakurai, Y. *J Controlled Release* 1993, 24, 119.
- Jeong, B.; Bae, Y. H.; Lee, D. S.; Kim, S. W. *Nature* 1997, 388, 860.
- Yasuda, H.; Aludin, M. S.; Kitamura, N.; Tanabe, M.; Sirahama, H. *Macromolecules* 1999, 32, 6047.
- Bradley, M. C.; Brain, A. J.; Maren, P.; Marc, A. H.; William, B. T. *Macromolecules* 2000, 33, 3970.
- Jain, R. A. *Biomaterials* 2000, 21, 2475.
- Jeong, B.; Kim, S. W.; Bae, Y. H. *Adv Drug Delivery Rev* 2002, 54, 37.
- Liggins, R. T.; Burt, H. M. *Adv Drug Delivery Rev* 2002, 54, 191.
- Kricheldorf, H. R.; Kreiser-Saunders, I.; Boettcher, C. *Polymer* 1995, 36, 1253.
- Ovitt, T. M.; Coates, G. W. *J Am Chem Soc* 1999, 121, 4072.
- Ishiku, U. S.; Pang, K. W.; Lee, W. S.; Ishak, Z. A. M. *Eur Polym J* 2002, 38, 393.
- Sanders, L. M.; Kent, J. S.; McRea, G. I.; Vickery, B. H.; Tice, T. R.; Lewis, D. H. *J Pharm Sci* 1984, 73, 1294.
- Miyajima, M.; Koshika, A.; Okada, J.; Ikeda, M. *J Controlled Release* 1999, 61, 295.
- Choi, N. S.; Kim, C. H.; Cho, K. Y.; Park, J. K. *J Appl Polym Sci* 2002, 86, 1892.
- Liu, L. J.; Li, S. M.; Garreau, H.; Vert, M. *Biomacromolecules* 2000, 1, 350.
- Deng, F.; Bisht, K. S.; Gross, R. A.; Kaplan, D. L. *Macromolecules* 1999, 32, 5159.
- Kim, J. K.; Park, D. J.; Lee, M. S.; Ihn, K. J. *Polymer* 2001, 42, 7429.
- Jeon, O.; Lee, S. H.; Kim, S. H.; Lee, Y. M.; Kim, Y. H. *Macromolecules* 2003, 36, 5585.
- Broz, M. E.; VanderHart, D. L.; Washburn, N. R. *Biomaterials* 2003, 24, 4181.
- Dunne, M.; Corrigan, O. I.; Ramtoola, Z. *Biomaterials* 2000, 21, 1659.
- Korhonen, H.; Helminen, A.; Seppala, J. V. *Polymer* 2001, 42, 7541.
- Finne, A.; Albertsson, A. C. *Biomacromolecules* 2002, 3, 684.
- Cai, Q.; Zhao, Y. L.; Bei, J. Z.; Xi, F.; Wang, S. G. *Biomacromolecules* 2003, 4, 828.
- Zhao, Y. L.; Shuai, X. T.; Chen, C. F.; Xi, F. *Chem Mater* 2003, 15, 2836.
- Dong, C. M.; Qiu, K. Y.; Cu, Z. W.; Feng, X. D. *Macromolecules* 2001, 34, 4691.
- Cui, Y. J.; Tang, X. Z.; Huang, X. B.; Chen, Y. *Biomacromolecules* 2003, 4, 1491.
- Bosman, A. W.; Janssen, H. M.; Meijer, E. W. *Chem Rev* 1999, 99, 1665.
- Grayson, S. K.; Frechet, J. M. J. *Chem Rev* 2001, 101, 3819.
- Trollsas, M.; Hedrick, J. L. *J Am Chem Soc* 1998, 120, 4644.
- Tomalia, D. A.; Baker, H.; Dewald, J. R.; Hall, M.; Kallos, G.; Martin, S.; Roeck, J.; Ryder, J.; Smith, P. *Polym J (Tokyo)* 1985, 17, 117.
- Trollsas, M.; Atthof, B.; Wursch, A.; Hedrick, J. L.; Pople, J. A.; Gast, A. P. *Macromolecules* 2000, 33, 6423.
- Lepoittevin, B.; Matmour, R.; Francis, R.; Taton, D.; Gnanou, Y. *Macromolecules* 2005, 38, 3120.
- Comanita, B.; Noren, B.; Roovers, J. *Macromolecules* 1999, 32, 1069.
- Roovers, J.; Zhou, L. L.; Toporowski, P. M.; Vanderzwan, M.; Iatrou, H.; Hadjichristidis, N. *Macromolecules* 1993, 26, 4324.
- Hedden, R. C.; Bauer, B. J.; Smith, A. P.; Grohn, F.; Amis, E. *Polymer* 2002, 43, 5473.
- Hedden, R. C.; Bauer, B. J. *Macromolecules* 2003, 36, 1829.
- Claesson, H.; Malmström, E.; Johansson, M.; Hult, A. *Polymer* 2002, 43, 3511.
- Hedrick, J. L.; Trollsas, M.; Hawker, C. J.; Atthoff, B.; Claesson, H.; Heise, A.; Miller, R. D.; Mecerreyes, D.; Jerome, R.; Dubois, P. *Macromolecules* 1998, 31, 8691.
- Nunez, E.; Ferrando, C.; Malmstrom, E.; Claesson, H.; Werner, P. E.; Gedde, U. W. *Polymer* 2004, 45, 5251.
- Zhao, Y. L.; Cai, Q.; Jiang, J.; Shuai, X. T.; Bei, J. Z.; Chen, C. F.; Xi, F. *Polymer* 2002, 43, 5819.
- Maiti, P.; Yamada, K.; Okamoto, M.; Ueda, K.; Okamoto, K. *Chem Mater* 2002, 14, 4654.
- Choi, Y. K.; Bae, Y. H.; Kim, S. W. *Macromolecules* 1998, 31, 8766.
- Wang, F.; Bronich, T. K.; Kabanov, A. V.; Rauh, R. D.; Roovers, J. *Bioconjugate Chem* 2005, 16, 397.
- Dell'Erba, R.; Groeninckx, G.; Maglio, G.; Malinconico, M.; Migliozi, A. *Polymer* 2001, 42, 7831.
- Crescenzi, V.; Manzini, G.; Calzolari, G.; Borri, C. *Eur Polym J* 1972, 8, 449.
- Fischer, E. W.; Sterzel, H. J.; Wegner, G. K.-Z. *Z. Polymer* 1973, 251, 980.
- Sarasua, J. R.; Prud'homme, R. E.; Wisniewski, M.; Le Borgne, A.; Spassky, N. *Macromolecules* 1998, 31, 3895.
- Sarasua, J.-R.; Rodriguez, N. L.; Arraiza, A. L.; Meaurio, E. *Macromolecules* 2005, 38, 8362.